Journal of Groundwater Science and Engineering
ISSN 2305-7068
Indexed by ESCI CABI CSA
Scopus GeoRef AJ CNKI

Development and application of multi-field coupled high-pressure triaxial apparatus for soil

Xiu-yan Wang, Lin Sun, Shuai-wei Wang, Ming-yu Wang, Jin-qiu Li, Wei-chao Sun, Jing-jing Wang, Xi Zhu, He Di

Citation:
Wang XY, Sun L, Wang SW, *et al*. 2023. Development and application of multi-field coupled high-pressure triaxial apparatus for soil. Journal of Groundwater Science and Engineering, 11(3): 308-316.

View online: https://doi.org/10.26599/JGSE.2023.9280025

Journal of Groundwater Science and Engineering 11(2023) 308–316

Journal homepage: http://gwse.iheg.org.cn

Research Paper

Development and application of multi-field coupled high-pressure triaxial apparatus for soil

Xiu-yan Wang[1*], Lin Sun[1], Shuai-wei Wang[1], Ming-yu Wang[2], Jin-qiu Li[1], Wei-chao Sun[1], Jing-jing Wang[1], Xi Zhu[1], He Di[1]

[1] *Institute of Hydrogeology and Environmental Geology*, *Chinese Academy of Geological Sciences*, *Shijiazhuang* 050061, *China*.
[2] *SuperMap Software Co.*, *Ltd. Beijing* 100000, *China*.

Abstract: The increasing severity of ground subsidence, ground fissure and other disasters caused by the excessive exploitation of deep underground resources has highlighted the pressing need for effective management. A significant contributing factor to the challenges faced is the inadequacy of existing soil mechanics experimental instruments in providing effective indicators, creating a bottleneck in comprehensively understanding the mechanisms of land subsidence. It is urgent to develop a multi-field and multi-functional soil mechanics experimental system to address this issue. Based soil mechanics theories, the existing manufacturing capabilities of triaxial apparatus and the practical demands of the test system, a set of multi-field coupled high-pressure triaxial system is developed tailored for testing deep soils (at depths of approximately 3 000 m) and soft rock. This system incorporates specialized design elements such as high-pressure chamber and horizontal deformation testing devices. In addition to the conventional triaxial tester functions, its distinctive feature encompass a horizontal deformation tracking measuring device, a water release testing device and temperature control device for the sample. This ensemble facilitates testing of horizontal and vertical deformation water release and other parameters of samples under a specified stress conditions, at constant or varying temperature ranging from −40°C–90°C. The accuracy of the tested parameters meets the requirements of relevant current specifications. The test system not only provides scientifically robust data for revealing the deformation and failure mechanism of soil subjected to extreme temperature, but also offers critical data support for major engineering projects, deep exploration and mitigation efforts related to soil deformation-induced disaster.

Keywords: Multi-field coupled triaxial test; High and low temperature; Horizontal deformation; Compressed water release

Received: 15 Nov 2022/ Accepted: 09 Jul 2023/ Published: 15 Sep 2023

Introduction

Geotechnical testing constitutes a crucial component of engineering geology, soil mechanics, geotechnics and other relevant fields, offering valuable insights into soil structure and mechanical properties. The range and density of parameters tested by a triaxial apparatus directly reflect the level of research objectives. With population growth and the rapid development of urbanisation, resource utilization has also been accelerated, the exploitation of deep groundwater and petroleum resources has led to varying degrees of ground subsidence, ground cracks and associated economic losses (Ha et al. 2021; Gao et al. 2019; Luo et al. 2019; Bagheri-Gavkosh et al. 2021; Haley et al. 2022; He et al. 2019). However, the mechanics of soil deformation and failure remain insufficiently understood, impeding effective geological disaster prevention and control. A key factor contributing

*Corresponding author: Xiu-yan Wang, *E-mail address*: wxiuyan-9948@163.com

DOI: 10.26599/JGSE.2023.9280025

Wang XY, Sun L, Wang SW, et al. 2023. Development and application of multi-field coupled high-pressure triaxial apparatus for soil. Journal of Groundwater Science and Engineering, 11(3): 308-316.

to this gap is the limited scope of effective parameters provided by existing testing equipment, hindering scientific research and practical engineering. The need for a multi-field coupled triaxial test system has becoming pressing.

Traditional triaxial testers are mainly used to yield mechanical parameters such as stress, strain and strength of rock and soil (Burland, 2007), with a range that is often limited to 0.6 MPa. Major engineering projects have made some improvement in enhancing the range and multifunctionality, mainly demonstrated by the following aspects: (1) The development of high-range triaxial testers is well established (Chen et al. 2019); for example, GDS Geotechnical Testing Instruments in the UK offers a triaxial instrument with a maximum vertical pressure of 500 KN, primarily for rock testing; (2) Mao et al. (2015) employed image processing techniques to study local deformation and damage evolution in triaxial soil samples (Yang et al. 2019), yielding substantial insights; (3) Sultan et al. (2002) elevated the temperature capabilities of GDS triaxial testers to 100°C, and Hu et al (2015) conducted trial or experimental studies on temperature-controlled unidirectional triaxial testers (Xiao et al. 2020; Xiong et al. 2022). Despite considerable advancements in testing functions and the pivot role they play in scientific research and engineering construction, current triaxial testers still require enhancements to address geotechnical hazards caused by deep probing, mining and deep exploration, especially under temperature-related environmental conditions. Additionally, certain parameter indicators remain underrepresented, including: (1) the amount of water released during soil sample compression; (2) horizontal deformation during soil sample compression; and (3) test parameters under changing temperature field conditions or constant temperature.

Based on the theories of geomechanics, engineering geology, hydrogeology, combined with previous findings (Yin et al. 2019; Deng and Deng, 2019) and comprehensive technologies such as motor-driven technology, automatic control technology, and laser measurement technology, this study has developed a set of multi-field coupled high-pressure triaxial testing system. This innovative apparatus not only facilitates traditional triaxial compression and static lateral pressure coefficient tests, but also accommodates unresolved parameters like water release and horizontal deformation of soil triaxial. It also incorporates a temperature range spanning from −40°C to 90°C. This test system can provide scientifically robust parameters essential for addressing geological disasters such as ground settlement and ground cracks caused by exploration and exploitation of deep underground resources in varying temperature environments. It will supply reliable parameters for the execution of major projects from soil to soft rock, playing an important role in advancing the geosciences disciplines.

1 Main structure of the apparatus

The multi-field coupled high-pressure triaxial test system combines vertical stress field, vertical and horizontal strain field, infiltration field and temperature field. The system consists of the following key components: (1) triaxial testing device: Primarily composed of servo-controlled loading host and three high-pressure triaxial pressure chambers; (2) high and low temperature control unit; (3) horizontal deformation test device; (4) data acquisition and computer processing unit, including digital multi-channel stress, displacement, peripheral pressure counterpressure, pore water pressure, pore water volume and other parameters, which are detected by sensors and transmitted to the control system for analysis. The main structure of the multi-field coupled triaxial test system is depicted in Fig. 1, while its physical setup is presented in Fig. 2.

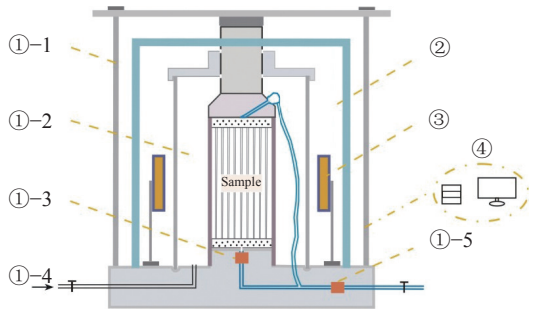

Fig. 1 Schematic diagram of main structure with multi-field coupled high-pressure triaxial system
①-1 Loading frame ①-2 Pressure chamber ①-3 Pore water pressure testing device ①-4 Liquid inlet ①-5 Seepage device ② Temperature control device ③ Horizontal deformation testing device ④ Data acquisition and processing device

2 Main features of the apparatus

The multi-field coupled high-pressure triaxial test system serves not only as a conventional triaxial tester but also facilitate fully automatic static triaxial testing, constant rate consolidation testing, K_0 testing, and more. Additionally, it can measure horizontal deformation, pore water pressure, pore water volume and other parameters. With the

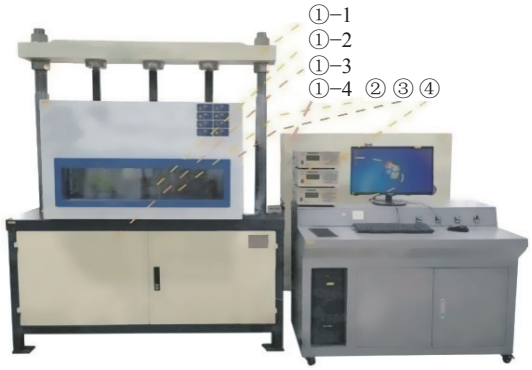

Fig. 2 Photo of multi-field coupled high-pressure triaxial test system

①-1 Loading Frame ①-2 Pressure chamber ①-3 Servo host ①-4 Water circuit control device ② Horizontal deformation testing device ③ High and low temperature control device ④ Data acquisition and processing device

integration of vertical strain field, horizontal strain field, infiltration field and temperature field within a single system, its applicability is greatly broadened.

2.1 Multi-functional high-pressure triaxial test apparatus

The core component of the test system is the multi-functional high-pressure triaxial test apparatus, as shown in Fig. 1. This apparatus has several key enhancements compared to the conventional triaxial testers: Firstly, the vertical pressure and circumferential pressure of the triaxial tester are increased; secondly, the measurement device for the pore water volume and pore water pressure parameter are introduced. Details are as follows:

(1) Servo host

The servo host comprises a servo motor, reducer and other components. Axial pressure, loading speed, vertical deformation and other data are transmitted to the control system through axial stress sensor and grating displacement meter. The axial pressure capacity of the pressure frame of the servo host is ≤ 50 KN, with a lifting speed range of 0.002 mm/min to 4.5mm/min, and an axial stroke range of 0 to 100 mm. The servo host applies pressure to the sample, inducing the corresponding deformation.

(2) Triaxial pressure chamber and pressure-volume change device

The triaxial pressure chamber can withstand up to 10 MPa of peripheral pressure and is capable of high and low temperature operations. It accommodates sample sizes of Φ39.1×80.0 mm and Φ61.8×125.0 mm. The pressurizing medium is an aqueous ethylene glycol solution designed to withstand simultaneous high and low temperatures.

Pressure-volume change device precisely controls peripheral and counterpressure volume changes via digital pressure/volume controllers.

(3) Pore water pressure and pore water volume measurement devices

A pore water pressure device (Fig. 1①-3) is introduced to measure pore water pressure parameter during triaxial consolidation undrained shear tests or compression tests. To test the pore water volume, a seepage device is added within the sample's pore water overflow (Fig. 1①-5). This device measures pore water volume during triaxial consolidation, drainage shear tests (CU) or compression tests, providing real-time data during the sample's triaxial compression process. This parameter signifies the amount of pore water released during soil deformation, which is crucial for accurately estimating resources volumes such as groundwater or oil.

2.2 Temperature control device

The temperature control device is placed outside the triaxial pressure chamber, as shown in Fig. 1①-2, Fig. 2③. A glass window is installed on the front and side of the temperature box. The temperature box adheres to China's high and low temperature chamber technical standards, ranging from −40°C to 90°C. Temperature changes occur at a rate of 1.0°C/min to 3.0°C/min during testing, with cooling rates of 0.8°C/min to 2.0°C/min. Rapid temperature changes of 3.0°C/min to 5.0°C/min can also be selected.

This temperature control device simulates geothermal or permafrost conditions, supplying experimental parameters for soil deformation and damage under specific temperature scenarios. It enhances the system's practical value (Wang et al. 2020; Vu et al. 2019; Xi et al. 2020; Chen et al. 2021; Xiao et al. 2021; Zhao et al. 2022; Deng and Deng, 2019).

2.3 Horizontal deformation measurement device

Horizontal deformation tracking device mainly consists of a line laser measurement probe (Japan KEYENCE LJ-V7200). The probe can be fixed around the pressure chamber or outside the temperature box window to measure the horizontal deformation parameter of the sample, as shown in Fig. 1③. The probe operates within the tem-

perature range of 0°C to +45°C. When measuring the sample's horizontal deformation under conditions of 0°C–+45°C, the probe is affixed to the pressure chamber during testing. For other temperature conditions, the test probe is positioned outside the temperature box window. The probe's placement falls within its effective testing range.

This device incorporates four test probes that measure data at the outer edges of four vertical lines in the horizontal direction. When no pressure is applied to the sample, the probe firstly measures the horizontal distance from a linear signal area to the sample's vertical line, providing an initial value expressed as various point spacings: X_{01}, $X_{02}\cdots X_{060}$. Upon applying pressure to the sample, changes in time result in vertical deformation and observable horizontal deformation within the sample. The horizontal distance from the signal area to the sample then changes to X_{11}, $X_{12}\cdots X_{160}$, X_{21}, $X_{21}\cdots X_{260}$. This change in horizontal distance corresponds to the samples horizontal deformation - X_1, $\triangle X_2\cdots\triangle X_{60}$. The number of test points and intervals can be adjusted (the effective height of in the test area is 6.0 cm, the test interval is set as 1.0 mm). The single probe test data is illustrated in Table 1. By utilizing imaging and simulation techniques to reconstruct the sample's spatial deformation, the horizontal deformation at a specific moment can be determined. The testing process is depicted in Fig. 3-1, and the horizontal deformation data of the sample from a single probe test is presented in Fig. 3-2.

The main purpose of the horizontal deformation measurement device is to acquire horizontal deformation parameters of the sample under specific vertical stress conditions. This information holds great value for researching and predicting deformation-related disasters, such as ground cracks and landslides.

2.4 Data acquisition and processing device and its accuracy

The data acquisition and processing device consists of three main components: (1) a multifunctional high-pressure triaxial test device, encompassing communication interfaces and lines, axial stress (σ_1), peripheral pressure counterpressure (σ_3), digital displacement sensors RS-50A (vertical deformations), vertical pressure sensors, pore water pressure (u), pore water flow (Q) and other parameters; (2) the temperature control device, automatic control unit located on the side of the tempe-

Table 1 Test accuracy of the developed system

Category	Data/mm			
Distance from the probe to the sample	X_{01}	X_{02},	…	X_{060}
1st data	X_{11}	X_{12},	…	X_{160}
1st horizontal deformation data	$\triangle X_{11}$	$\triangle X_{12}$	…	$\triangle X_{160}$
2nd data	X_{21}	X_{21}	…	X_{260}
2nd horizontal deformation data	$\triangle X_{21}$	$\triangle X_{22}$	…	$\triangle X_{260}$
…	…	…		…
nth data	X_{n1}	X_{n2}	…	X_{n60}
Nth horizontal deformation data	$\triangle X_{n1}$	$\triangle X_{n2}$	…	$\triangle X_{n60}$

Note：($\triangle X_{n1}= X_{n1}-X_{01}$)

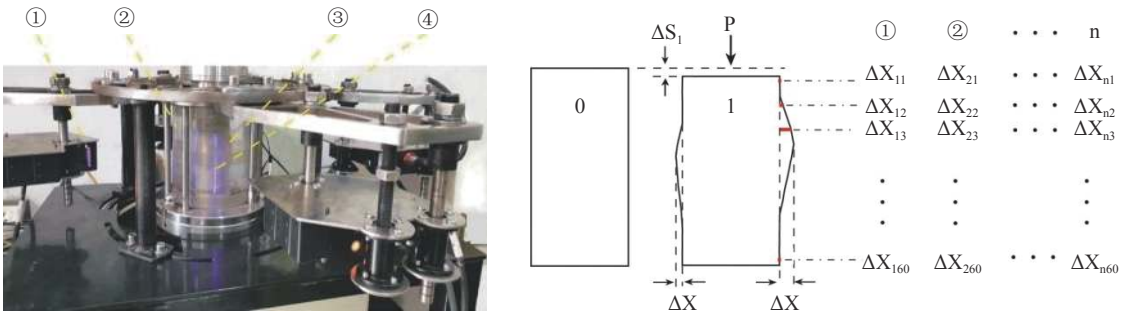

Fig. 3 The device for testing horizontal deformation of sample

① Line laser measuring probe and signal area ② Pressure chamber ③ Sample ④ Horizontal deformation test area

①, ②, ⋯n are the horizontal deformation results of the 1st, 2nd, ⋯nth test sample, respectively.

rature control box; (3) acquisition and storage control for sample horizontal radial deformation (△X) parameters. Through specialized interfaces and standard timing, the computer connects data acquisition and processing from these three components to execute automatic tests and generate outputs. The power supply requirement is 220 at 50 HZ.

The multifunctional triaxial test system can automatically conduct tests on parameters such as triaxial strength, compression, water release, horizontal deformation of samples under temperature environment ranging from −40°C to 90°C. It can also collect, process, and generate curves and corresponding test reports in accordance with relevant regulations. The time interval for collecting test parameters are adjustable.

Regarding system accuracy, the multi-field coupled triaxial system measures test parameters such as vertical pressure, vertical deformation, pore water pressure, temperature, etc. The test range and accuracy of each parameter are presented in Table 2, and the accuracy of each parameter is aligned with current national standards.

2.5 Basis for the pressure and temperature settings of the test system and application scope

North China, situated within the North China fracture basin, is one of the most important economic zones in China, endowed with rich groundwater (geothermal), oil and other resources. The fracture basin from the Taihang Mountains to the east of the Quaternary and Tertiary soil layers, characterized by greater depth and thickness. The Upper Tertiary Guantao Formation geothermal storage in the basement is at depths ranging from 700 m to 2 870 m. The temperature gradient of the ground ranges from 2°C to 3.7°C per 100 m, and wellhead water temperatures are between 35°C and 85°C (Rao et al. 2023; Wang et al. 2017). In this region, due to the scarcity of surface freshwater and the poor quality of shallow groundwater, deep groundwater serves as the primary water source for industry and agriculture. Additionally, hot water resources are being developed and utilised as a clean energy. However, over-exploitation of deep groundwater (geothermal) and other resources has led to the formation of groundwater exploitation cones in Tianjin, Cangzhou, and Beijing, and has caused severe disasters such as ground subsidence and geocracks (Gao et al. 2019; Zhou et al. 2020), which have yet to be effectively managed. Existing geomechanical testing equipment fail in providing effective data.

Under these circumstances, and considering the limited availability of testing devices for studying deep soil in temperature environments, as well as limited parameters, the decision to set sub-zero temperatures (primarily due to unpredictable factors in permafrost projects) was made. These testing conditions might include scenarios involving construction and maintenance under freezing conditions, where temperatures could be as low as −25°C to −30°C or even lower. Consequently, the developed system device parameters are set as follows: Axial pressure of the main unit ≤ 50 KN, peripheral pressure of 10 MPa, temperature range of −40°C to 90°C (considering the the underwater self-weight stress of the soil body, approximately 1.2 MPa/100 m for a sample size of Φ39.1 mm). These settings are designed to accommodate the soil testing and research needs within a burial depth of 3 000 meters.

The test system is suitable for conducting triaxial compression, shear, water release, lateral deformation and other parameters of the soil within a temperature environment ranging from −40°C to 90°C and at burial depths of about 3 000 meters.

3 System verification and discussion

3.1 System verification

The test sample was extracted from clay in Hengshui city, Hebei province. The sample's burial depth is 79.10 m, with a superconsolidation ratio of 1.04. Its specific gravity (G) is 2.74, density (ρ) is 2.05 g/cm^3, water content (W) is 27.3%, satu-

Table 2 Test accuracy of the developed system

Index	Vertical pressure	Confining pressure	Vertical deformation	Horizontal deformation	Pore water pressure	Pore water volume	Temperature
Unit	P/kN	$б_3$/MPa	S/mm	X/mm	u/MPa	Q/mL	°C
Range	50	10	30	10	3	100	−40–90
Accuracy	0.01%F.S	0.01%F.S	0.001	±0.044	0.01% F.S	0. 01	±0.10
Note			Grating displacement gauge	Line laser scanning			Constant or changing temperature

ration (Sr) is 100%, liquid limit (W_L) is 41.3%, plastic limit (W_P) is 23.4%, plasticity index (I_p) is 18.1 and liquidity index (I_L) is 0.22. The sample's dimensions are as follows: Height=8.00 cm, area= 12.00 cm^2. Given the sample's burial depth and the temperature environment, the test conditions were set as follow: Peripheral pressure(σ_3) = 100 Kpa, shear rate = 0.012 mm/min, and constant temperature of 25°C. Utilizing the developed test system, a multi-field coupled triaxial consolidation and drainage test was conducted on the sample. The test maintained a peripheral pressure of 100 kPa while incrementally increasing axial stress (σ_1-σ_3) to deform the sample until failure.

During the test, it was observed that as axial stress (σ_1-σ_3) increased, the vertical deformation (S) of the soil sample increased correspondingly. Simultaneously, the amount of water released from the sample (Q) and the horizontal deformation of the four measurement lines (X) were changing. The main steps of the test are illustrated in Fig. 4, and the relationship between the amount of water released from the sample (Q) and the vertical deformation of the sample (S) is presented in Fig. 4(1). The axial stresses (σ_1-σ_3) were set at 114 KPa, 203 KPa, and 300 KPa respectively, with corresponding test parameters for characteristic points listed in Table 3. Furthermore, a measurement line displaying the most significant change in horizontal deformation, along with a schematic representation of the situation are depicted in Fig. 4(2) - Fig. 4(3). The test results show that,

Under the influence of constant temperature 25°C and rapid increase in effective stress, the vertical deformation of the sample demonstrates a positive correlation with the amount of water release and horizontal deformation. The test data results can be categorized into three phases (Fig. 4 (1)):

Phase Ⅰ: This phase corresponds to a rapid change in vertical deformation (stress P<40 KPa).

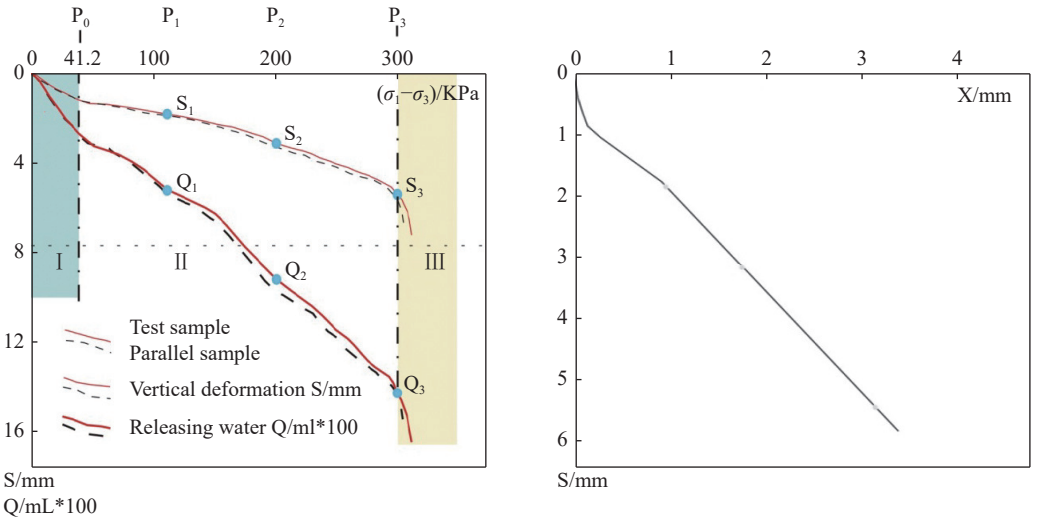

(1) Sample vertical deformation and water release process

(2) Relationship between vertical deformation (S/mm) and horizontal deformation (X/mm)

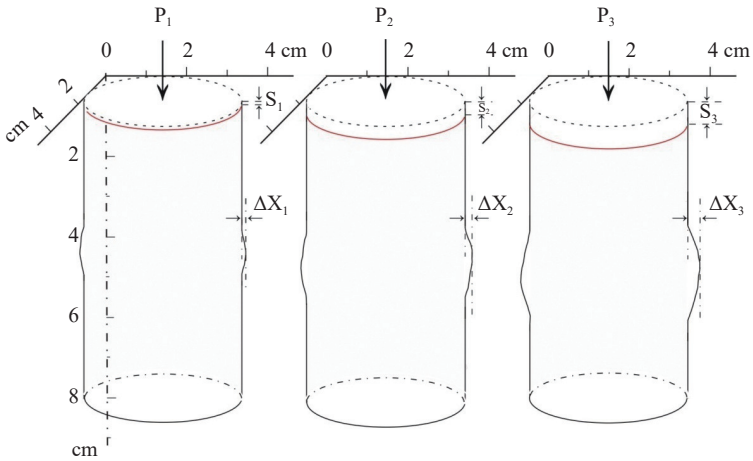

(3) Horizontal deformation process of sample

Fig. 4 Main process of multi-field coupled triaxial test

Table 3 Soil parameters measured under the condition of multi field coupling

Effective stress	Vertical deformation	The amount of water released	Maximum horizontal deformation	Volume of water released/volume of deformation
Kpa	S /mm	V /cm^3	X /mm	%
114	1.864	0.052 3	0.982	2.340
203	3.160	0.091 8	1.745	2.421
300	5.440	0.142 0	3.137	2.175

It primarily arises due to the stress unloading rebound during the sampling process, with minimal horizontal deformation. This phase also indicates that the release of water from the soil sample lags behind its vertical deformation.

Phase II: In this stage, characterized by a smooth change (40 KPa ≤ P < 300 KPa), the sample's vertical deformation, water release and horizontal deformation all exhibit smooth, gradual increases.

Stage Ⅲ : A rapid change stage (P ≥ 300 KPa), indicates that when stress levels reach P ≥ 300 KPa, the sample undergoes rapid deformation and water release, eventually leading to its destruction. Notably, the deformation volume exhibited by the clay is primarily attributed to pore compression and lateral deformation. The volume of water released during compression is minimal, with the water release volume/vertical deformation volume ratio being < 2.421%, indicating that over-exploitation of groundwater serves as a significant contributor not only to ground subsidence, but also to ground cracks.

Through a comparison test conducted with parallel samples under identical conditions at the laboratory of Hebei CNNC Geotechnical Engineering Company (using the high-pressure triaxial instrument produced by Beijing Huakan Technology Co., Ltd.), the changes in vertical deformation and pore water volume of soil samples were found to align with the patterns observed in the developed system. The verification of the comparative test results, as depicted in Fig. 4(1), indicated an error of vertical deformation ≦5.3% and an error of water release ≤6.3%. Such discrepancies in are attributed to variations in soil sample uniformity and minor inconsistencies in temperature control. Overall, the test results confirm the accuracy and reliability of the developed test system.

3.2 Discussions

(1) The testing of pore water volume and pore water pressure parameters within the system is applicable to saturated soil drainage compression tests and consolidated drainage shear tests (CU) under specific temperature conditions. During these test, it's important to note that only one parameter of the sample can be tested at a time: Either the pore water volume or the pore water pressure. Researcher can collectively make a decision on which parameter to prioritize for testing.

(2) Table 3 provides insight into the relationship between water release volume and deformation volume of the sample under the constant temperature of 25°C. The observed range of water release volume/deformation volume, spanning from 2.175% to 2.421%, highlights two significant aspects. Firstly, it signifies that the water release capacity of the sample is very low. Secondly, it indicates that over 95% of the vertical deformation volume of the sample is converted to lateral deformation. This may be the fundamental cause for the frequent occurrence of ground cracks around areas of ground settlement. Moreover, this observation highlights the importance of incorporating a "horizontal deformation measurement device" to assess the horizontal deformation parameters of the sample in this system.

4 Conclusions

The developed system is a multi-field coupled soil mechanics testing device, encompassing vertical stress field, vertical deformation field, horizontal deformation field, pore water infiltration field and temperature field. Its technical attributes are as follows:

(1) This test system is suitable for simulating triaxial stress conditions on soil at depth reaching 3 000 metres, while accommodateing a temperature range of −40°C to 90°C. It serves as a robust resource for gathering scientific data parameters that facilitate an in-depth exploration of soil deformation and failure mechanism. Furthermore, the system contributes to the development of deep resource exploration, engineering construction and other significant projects.

(2) The integration of testing parameters for soil pore water release volume and water release pressure within the device offers the means to comprehensively analyze and study the relationship between deformation volume and pore water during

the triaxial compression process. This capability extends to investigating the mechanism of joint infiltration of soil deformation. Moreover, the system aids in accurately calculating the quantities of groundwater, oil and other valuable resources.

(3) The device can directly test the horizontal deformation parameters of the sample during the triaxial compression process, which can provide effective parameters for the forecast and prediction of ground cracks and ground collapse disasters caused by underground space development, resource development and other projects.

Acknowledgements

This study was supported by National Natural Science Foundation (No. 41272301 and No.42007171); Nature Fund of Hebei (No.D2021504034) and Chinese Academy of Geological Sciences (No. YYWF201628).

References

Bagheri-Gavkosh M, Hosseini SM, Ataie-Ashtiani B, et al. 2021. Land subsidence: A global challenge. The Science of the Total Environment, 778: 146193. DOI：10.1016/j.scitotenv.2021.146193.

Burland J. 2007. Terzaghi: Back to the future. Bulletin of Engineering Geology and the Environment, 66(1): 29−33. DOI：10.1007/s10064-006-0083-9.

Chen ZQ, He C, Xu GW, et al. 2019. A case study on the asymmetric deformation characteristics and mechanical behavior of deep-buried tunnel in phyllite. Rock Mechanics and Rock Engineering, 52(11): 4527−4545. DOI：10.1007/s00603-019-01836-2.

Chen SM, Liu FT, Zhang Z, et al. 2021. Changes of groundwater flow field of Luanhe River Delta under the human activities and its impact on the ecological environment in the past 30 years. China Geology, 4: 455−462. DOI：10.31035/cg2021060.

Deng Y, Deng HC. 2019. Experimental study on failure criterion of deep tight sandstone under coupling effects of temperature and pressure. Arabian Journal of Geosciences, 12(18): 575. DOI：10.1007/s12517-019-4729-x.

Gao ML, Gong HL, Li XJ, et al. 2019. Land subsidence and ground fissures in Beijing capital international airport (BCIA): Evidence from quasi-PS InSAR analysis. Remote Sensing, 11(12): 1466. DOI：10.3390/rs11121466.

Ha D, Zheng G, LoÃiciga HA, et al. 2021. Long-term groundwater level changes and land subsidence in Tianjin, China. Acta Geotechnica, 16(4): 1303−1314. DOI：10.1007/s11440-020-01097-2.

Haley M, Ahmed M, Gebremichael E, et al. 2022. Land subsidence in the texas coastal bend: Locations, rates, triggers, and consequences. Remote Sensing, 14(1): 192. DOI：10.3390/rs14010192.

He XC, Yang TL, Shen SL, et al. 2019. Land subsidence control zone and policy for the environmental protection of Shanghai. International Journal of Environmental Research and Public Health, 16(15): 2729. DOI：10.3390/ijerph16152729.

Hu B, Gong BW, Tong J, et al. 2015. Development and application of unilateral freezing triaxial apparatus for freeze-thaw cycle. Journal of Yangtze River Scientific Research Institute, 32(2): 128−132. (in Chinese) DOI：10.3969/j.issn.1001-5485.2015.02.026.

Luo G, Pan SK, Zhang YL, et al. 2019. Research on establishing numerical model of geo material based on CT image analysis. EURASIP Journal on Image and Video Processing, 2019(1): 36. DOI：10.1186/s13640-019-0421-z.

Mao LT, Yuan ZX, Lian XY, et al. 2015. Measurement of 3d strain field in red stone sample under uniaxial compression with computer tomography and digital volume correlation method. Chinese Journal of Rock Mechanics and Engineering, 34(1): 21−30. (in Chinese) DOI：10.13722/j.cnki.jrme.2015.01.003.

Nawir H, Apoji D, Ekawita R, et al. 2018. Axial and lateral small strain measurement of soils in compression test using local deformation transducer. Journal of Engineering and Technological Sciences, 50(1): 53−72. DOI：10.5614/j.eng.technol.sci.2018.50.1.4.

Rao S, Xiao HP, Wang ZT, et al. 2023. Geothermal Reservoir characteristics and geothermal resource evaluation of Guantao Formation in the Bohai Bay Basin. Natural Gas Industry, 43(5): 141−152. (in Chinese)

Sultan N, Delage P, Cui YJ. 2002. Temperature ef-

fects on the volume change behaviour of Boom clay. Engineering Geology, 64(2−3): 135−145. DOI：10.1016/s0013-7952(01)00143-0.

Vu TL, Bares J, Mora S, et al. 2019. Deformation field in diametrically loaded soft cylinders. Experimental Mechanics, 59(4): 453−467. DOI：10.1007/s11340-019-00477-4.

Wang GL, Zhang W, Lin WJ, et al. 2017. Research on formation mode and development potential of geothermal resources in Beijing-Tianjin-Hebei region. Geology in China, 44(6): 1074−1085. (in Chinese) DOI：10.12029/gc20170603.

Wang P, Liu EL, Zhi B, et al. 2020. A macro-micro viscoelastic-plastic constitutive model for saturated frozen soil. Mechanics of Materials, 147: 103411. DOI：10.1016/j.mechmat.2020.103411.

Xiao WJ, Yu G, Li HT, et al. 2021. Experimental study on the failure process of sandstone subjected to cyclic loading and unloading after high temperature treatment. Engineering Geology, 293: 106305. DOI：10.1016/j.enggeo.2021.106305.

Xiao WJ, Zhang DM, Wang XJ. 2020. Experimental study on progressive failure process and permeability characteristics of red sandstone under seepage pressure. Engineering Geology, 265: 105406. DOI：10.1016/j.enggeo.2019.105406.

Xi BP, Wu YC, Zhao YS, et al. 2020. Experimental investigations of compressive strength and thermal damage capacity characterization of granite under different cooling modes. Chinese Journal of Rock Mechanics and Engineering, 39(2): 286−300. (in Chinese) DOI：10.13722/j.cnki.jrme.2019.0782.

Xiong X, Gao F, Zhou KP, et al. 2022. Mechanical properties and strength evolution model of sandstone subjected to freeze–thaw weathering process: Considering the confining pressure effect. Mathematics, 10(20): 3841. DOI：10.3390/math10203841.

Yang SQ, Tian WL, Jing HW, et al. 2019. Deformation and damage failure behavior of mudstone specimens under single-stage and multi-stage triaxial compression. Rock Mechanics and Rock Engineering, 52(3): 673−689. DOI：10.1007/s00603-018-1622-y.

Yin TB, Li Q, Li XB. 2019. Experimental investigation on mode I fracture characteristics of granite after cyclic heating and cooling treatments. Engineering Fracture Mechanics, 222: 106740. DOI：10.1016/j.engfracmech.2019.106740.

Zhao XD, Lv ZY, Zhou Y, et al. 2022. Thermal and pore pressure gradient-dependent deformation and fracture behavior of saturated soils subjected to freeze-thaw. Bulletin of Engineering Geology and the Environment, 81(5): 188. DOI：10.1007/s10064-022-02693-0.

Zhou CF, Gong HL, Chen BB, et al. 2020. Land subsidence response to different land use types and water resource utilization in beijing-Tianjin-hebei, China. Remote Sensing, 12(3): 457. DOI：10.3390/rs12030457.